Colored reflectors to improve coincidence timing resolution of BGO-based time-of-flight PET detectors

Daehee Lee,

Simon R. Cherry,

Sun Il Kwon

Department of Biomedical Engineering, University of California, Davis, Davis, CA 95616, United States of America

Abstract

Time-of-flight (TOF) positron emission tomography (PET) detectors improve the signal-to-noise ratio of PET images by limiting the position of the generation of two 511-keV gamma-rays in space using the arrival time difference between the two photons. Unfortunately, bismuth germanate (BGO), widely used in conventional PET detectors, was limited as a TOF PET scintillator due to the relatively slow decay time of the scintillation photons. However, prompt Cerenkov light in BGO has been identified in addition to scintillation photons. Using Cerenkov photons for timing has significantly improved the coincidence timing resolution (CTR) of BGO. Based on this, further research on improving the CTR for a BGO-based TOF PET system is being actively conducted.

Wrapping materials for BGO pixels have primarily employed white reflectors to most efficiently collect scintillation light. White reflectors have customarily been used as reflectors for BGO pixels even after Cerenkov light began to be utilized for timing calculations in pixel-level experiments. However, when the arrival-time differences of the two 511-keV annihilations photons were measured with pure Cerenkov radiators, painting the lateral sides of the radiators black can improve CTR by suppressing the reflection of Cerenkov photons. The use of BGO for TOF PET detectors requires simultaneously minimizing scintillation loss for good energy information and suppressing reflected Cerenkov photons for better timing performance. Thus, reflectors for BGO pixels should be optimized for better timing and energy performance.

In this study, colored polytetrafluoroethylene (PTFE) tapes with discontinuous reflectance values at specific wavelengths were applied as a BGO reflector. We hypothesized that CTR could be enhanced by selectively suppressing reflected Cerenkov photons with an optimum colored reflector on the BGO pixel while minimizing scintillation photon loss. CTRs were investigated utilizing white and three colors (yellow, red, and green) PTFE tapes as a reflector. In addition, black-painted PTFE tape and enhanced specular reflector (ESR) film were investigated as reference reflector materials. When $3 \times 3 \times 20$ mm^3 BGO pixels were wrapped with the yellow PTFE reflector, the CTR was significantly improved to 365±5 ps from 403±14 ps measured with the conventional white PTFE reflector. Adequate energy information was still obtained with only

Corresponding author: Sun Il Kwon (sunkwon@ucdavis.edu).

4.1% degradation in light collection compared to the white reflector. Colored reflectors show the possibility to further improve CTR for BGO pixels with optimum reflectance design.

Keywords

1. Introduction

Bismuth germanate (BGO) initially received attention as a scintillator for early positron emission tomography (PET) scanners because of its high atomic number, high density, and short attenuation length for 511-keV gamma-ray photons (Moses 2007, Weber et al 2003). Time-of-flight (TOF) PET systems have since been developed to further increase the signal-to-noise ratio (SNR) of PET images, using the difference in the arrival time of two 511-keV annihilation photons (Karp et al., 2008; Surti, 2015; Vandenberghe et al., 2016). BGO was considered inappropriate for TOF PET because of its poor timing performance due to its moderate light yield and relatively long decay time (Karp et al., 2008; Surti & Karp, 2016). Newly developed fast scintillators with a high light yield, such as lutetium oxyorthosilicate (LSO) and lutetium-yttrium oxyorthosilicate (LYSO), have replaced BGO for TOF PET scanners (Leem et al., 2022; Ullah et al., 2016).

However, more recent work has shown that prompt Cerenkov photons arising from 511-keV gamma-ray interactions in BGO can be detected (Brunner & Schaart, 2017; Kwon et al., 2016). Besides prompt generation within a few picoseconds (ps), Cerenkov light has different characteristics from scintillation emission. Cerenkov photons are generated preferentially in the UV/blue wavelength range, while the scintillation photons of BGO are emitted over a wavelength range of 400 – 700 nm (Kwon et al., 2016). In addition, the number of produced Cerenkov photons is relatively small (< 20) compared to the number of scintillation photons of $\sim 8,000$ ph/MeV (Lecoq et al., 2010; Lowdon et al., 2019; Seitz et al., 2016). Unlike the isotropic emission of scintillation light, the first few Cerenkov photons have a gamma-ray-dependent directionality (Kratochwil et al., 2020; Kwon et al., 2019; Trigila et al., 2022). Based on these studies, additional research is being actively conducted to replace scintillators such as LSO and LYSO, which are currently employed in existing TOF PET systems, with BGO to further improve timing performance with this cost-effective detector material (Gundacker et al., 2020).

In conventional PET detectors, each scintillator pixel is wrapped with reflector material to collect more scintillation photons at the photosensor. More scintillation photons allow not only better energy information but also improvement in coincidence timing resolution (CTR) when scintillation photons are used for timing calculations. Thus, white reflectors, such as polytetrafluoroethylene (PTFE, also known as Teflon) tape, have been studied and used because they have high reflectance across all visible wavelengths (Janecek, 2012). Better timing and energy performance were achieved with such white reflectors (Janecek, 2012). On the other hand, when Cerenkov photons arising from pure Cerenkov radiator, which do not emit scintillation light, are used for timing, CTR is improved by suppressing reflections

of Cerenkov photons on the lateral sides of the Cerenkov radiator. This is because only a few tens of Cerenkov photons are produced by a 511-keV gamma photon, and travel-time dispersion of these photons degrades timing performance. Thus black tape or black paint has often been applied to the radiator (Dolenec et al., 2016). Therefore, to develop optimal TOF PET detectors using BGO, reflectors are required that suppress Cerenkov light reflection for better timing performance but simultaneously minimize scintillation-light loss during reflection for adequate energy information.

The reason why objects look different in color is that each material absorbs different wavelength ranges and reflects the rest. The reflection shows different discontinuous reflectance wavelengths according to the different colors of a material (Sattar, 2019). Because the scintillation and Cerenkov photons emitted in BGO have different emission spectra, we hypothesized that we could control reflectance for scintillation and Cerenkov photons in a BGO pixel separately. The high reflectance region of the colored reflector aims to minimize scintillation loss, while the low reflectance region aims to suppress Cerenkov photon reflection, which could deteriorate timing performance. In this study, we compared the performance of BGO wrapped with different colored PTFE tapes to verify the hypothesis. To provide a comparative perspective and reinforce our study, we adopt PTFE tape painted with black manually and an enhanced specular reflector (ESR) film (3M), which is known for its rapid decrease in reflectance under 400 nm (Roncali et al., 2017).

2. Materials and methods

2.1 BGO scintillators and colored PTFE tapes

A pair of polished $3 \times 3 \times 20$ mm^3 BGO pixels (Epic-crystal, China) was prepared. One of the two 3×3 mm^2 surfaces of each BGO pixel was optically coupled with NUV-HD MT silicon photomultipliers (SiPMs, FBK, Italy) (Merzi et al., 2023) using silicone optical grease (BC-630, Saint-Gobain, USA). The silicone optical grease has a flat transmittance of ~95 % for wavelengths down to 280 nm with a refractive index of 1.465 (Kwon et al., 2016; Romanchek et al., 2020). The NUV-HD MT SiPMs have a square cell pitch of 40 μm and an area of 3.2×3.2 mm^2. The surfaces of the NUV-HD MT SiPMs were left bare to minimize any loss of fast photons from the optically-coupled BGO pixels. The two SiPMs were optimally operated under an overvoltage of 16.5 V.

Figure 1 shows commercially available white, yellow, red, and green PTFE tapes (Taegatech, USA) which were used for the BGO pixel reflector. Each single-layer PTFE tape has a thickness of 81.28 μm. We measured the reflectance spectra for a single-layer and three-layers of these PTFE tapes with a UV-VIS-NIR spectrometer (Shimadzu 3700, Japan) using an integrating sphere. Three-layer PTFE tapes represent a practical reflector implementation for BGO pixels.

A pair of $3 \times 3 \times 20$ mm^3 BGO pixels was prepared and wrapped with different colored PTFE reflectors for the experiments. All five surfaces not in contact with the SiPM were wrapped in three layers of each colored PTFE tape, and energy and timing performances were measured. Each scintillator pixel wrapped in white or colored PTFE tape was secured

and tested in a holder made with a 3D printer (Object 260 Stratasys, Ltd, ISA) using an acrylate-based photopolymer (Verowhite).

2.2 Coincidence measurement setup

Figure 2 shows the experimental setup for the coincidence measurements. A ~3.3 MBq (~89.9 μCi) ^{22}Na point source centered 5 cm away from the two BGO pixels provided back-to-back 511-keV gamma rays to each BGO pixel wrapped with one of the reflectors.

Each SiPM coupled to BGO was connected to a custom preamplifier board to produce energy and timing signals. Each energy signal was connected to a NIM fan-in-fan-out (FIFO) module. One of the FIFO outputs was connected to a NIM coincidence logic module to determine coincidence events with a 20 ns coincidence timing window, and another FIFO output was connected to an oscilloscope (MSO72004C, Tektronix) to digitize each energy signal. A pole-zero (PZ)-cancelation circuit corrected the baseline at the customized board (Gola et al., 2013). Both timing signals were directly fed to the oscilloscope and used to calculate the CTR. The oscilloscope digitized energy and timing signals at 50 GS/s with 4 GHz bandwidths, respectively. A total of 50,000 events were acquired for CTR analysis in each experiment. The experiment was repeated with different colored PTFE reflectors, along with the reference black PTFE and ESR film reflectors. In this study, the optical grease was used for coupling between BGO pixel and ESR film (Gonzalez-Montoro et al., 2021). BGO pixels and SiPMs remained unchanged during the study to exclude the influence of any variation due to BGO pixel and SiPM changes on the measurements.

2.3 Data analysis

Each digitized energy signal was integrated for 2 μs to obtain energy information. The energy values were histogrammed to obtain an energy spectrum. The peak in the energy spectrum, corresponding to 511-keV being deposited in the BGO, was fitted with a single Gaussian for each of the reflectors measured. The energy resolution and relative light collection amount were calculated from the fitted Gaussian photopeak obtained from each measurement. The 434 keV peak corresponding to the bismuth X-ray escape was excluded from the fitting (Kwon et al., 2016; Szczesniak et al., 2013). Events within the full width at the tenth maximum (FWTM) around the 511 keV photopeak were selected for further timing analysis. In addition, to assess potential changes in CTR depending on the selected data, we also tested the energy within the full width at half maximum (FWHM) around the 511 keV photopeak for timing calculation (Kratochwil et al., 2020).

In timing analysis, the pick-off timing information of each digitized timing signal was computed using a leading edge threshold method after linear interpolation of each signal. A pick-off time difference between two timing signals of each event was computed and histogrammed to form a timing spectrum. The timing spectrum was fitted with a quadratic Gaussian function, and CTR values defined as the FWHM and FWTM were calculated in each measurement (Gonzalez-Montoro et al., 2022).

3.   Results and discussion

3.1   Reflectance of PTFE tapes

The reflectance of four different single-layer and three-layer colored PTFE tapes were measured with the integrating sphere and are shown in Figure 3(a) together with the emission spectra for the Cerenkov and scintillation photons emitted in a BGO pixel in Figure 3(b).

The white PTFE tape, widely used for PET detectors, showed continuous and high reflectance across a broad wavelength range, as expected. The three-layer white PTFE tape had a higher reflectance than the single-layer white PTFE tape in the measured wavelength range. For example, the reflectance was improved from 83 % to 91 % at 480 nm, at the peak scintillation light emission wavelength of BGO. On the other hand, yellow, red, and green-colored PTFE tapes showed quite different reflectance patterns depending on their colors. The reflectance of the yellow and red PTFE tape was sharply reduced at wavelengths below about 500 and 600 nm, respectively, while the reflectances at wavelength ranges above each cut-off wavelength were similar to the white tape. The reflectance of the green PTFE tape was reduced at wavelengths below around 750 nm, and its slope was slightly slower than those of yellow and red PTFE tapes. The reflectance of the green tape at the discontinuous wavelength region (>750 nm) was slightly higher than those of the yellow and red tapes. There was another reflectance region at about 550 nm, which was not observed for the yellow or red tapes. Interestingly, the reflectance of the discontinuous wavelength region, which showed low reflectance, remained unchanged even if the number of layers was increased from one to three. However, the reflectance of other regions in each colored tape increased with the number of layers and was similar to that of the white PTFE tape. Based on the above results, it was confirmed that the use of colored PTFE tapes could effectively reduce the reflection of photons in a specific wavelength range.

The reflectance of the black PTFE tape and ESR film, used as reference materials in this study, were sourced from reflectance values reported in other research studies (Dury et al., 2007; Gilbert & Haeberli, 2007; Gonzalez-Montoro et al., 2021).

3.2   Energy performance

Figure 4 represents the energy spectra from one of the SiPMs for each colored PTFE reflector obtained from a $3 \times 3 \times 20$ mm^3 BGO pixel, together with the results of the Gaussian fits, excluding the 434-keV escape peak. The 511-keV photopeak positions decreased in the order of ESR film, yellow, red, green, and black PTFE tapes (18.9 18.6, 16.6, 15.0, 12.4 and 2.8×10^3 [arbitrary units (a.u.)]) compared to the white (19.4×10^3 a.u.). These results agree well with the order of cut-off wavelengths of the reflectance measurement in Section 3.1. For the given scintillation light emission spectrum shown in Figure 3(b), as the cut-off wavelength increases due to the color, fewer scintillation photons are reflected and collected at the SiPM, decreasing the photo-peak positions. In Figure 3(a), the reflectance of the green PTFE tape is slightly higher than that of yellow or red tape. However, it was observed that the small difference in reflectance within the discontinuous wavelength regions did not significantly affect the photopeak position changes. One of the

reasons is that scintillation photons undergo many reflections. In a simulation study (Roncali et al., 2019), 58% of emitted scintillation photons underwent more than 15 reflections per photon in a $3 \times 3 \times 20$ mm^3 BGO crystal. Therefore, the cut-off wavelength was the most dominant factor in determining the photopeak position changes.

Table 1 summarizes the measured 511-keV peak position and energy resolution for each PTFE reflector including reference reflectors. As the light loss increased in the order of white, ESR film, yellow, red, green, and black PTFE reflectors, the the energy resolutions were respectively 21.4, 22.2, 23.2, 26.3, 23.6, and 28.0%, Interestingly, the energy resolution for the green PTFE reflector shows the similar range of the yellow PTFE reflector. The enhanced energy resolution for the green PTFE reflector could be attributed to high photon detection efficiency (PDE) of the NUV-HD MT SiPM and bumpy reflectance of green PTFE tape. The yellow PTFE reflector exhibited an energy resolution change of just 1.8%, the lowest energy resolution degradation among the three prepared colored PTFE tapes, while minimizing scintillation light loss. A significant reduction in energy photopeak was observed with the black PTFE reflector. Owing to its low light collection with low reflectance across all wavelengths, the black PTFE reflector exhimited the poorest energy resolution, nearly 28%, among all tested reflectors.

3.3 Timing performance

Coincidence timing spectra with each colored PTFE reflector applied to a $3 \times 3 \times 20$ mm^3 BGO pixel are shown in Figure 5. The noise level of the experimental setup remained consistent across all reflector cases as all other peripheral experimental setups were maintained except for the wrapped BGO pixels. We utilized a selected time pick-off threshold voltage of 4 mV, below one photoelectron. A 20-ps time bin was applied for each timing spectrum analysis.

Table 2 summarizes CTR values in FWHM and FWTM for each PTFE reflector with two different energy windows: FWTH and FWHM. The measured CTR with FWTM of the energy window between two BGOs wrapped with white PTFE reflectors was 403±14 ps in FWHM and 1309±31 ps in FWTM. When yellow PTFE reflectors were applied to the same BGO pixels, a CTR with FWTM of the energy window of 365±5 ps in FWHM and 1269±34 ps in FWTM was obtained. Notably, the CTR value in terms of FWHM was significantly improved by 38 ps compared to the result with the white PTFE reflector. Overall, all reflectors, including the black PTFE tape and ESR film, show better FWHMs in CTRs than the one with the white PTFE reflector. The CTR for the red reflector was 388±14 ps in FWHM and 1352±46 ps in FWTM, and the CTR of the green PTFE tape was 383±3 ps in FWHM and 1287±22 ps in FWTM. The black PTFE tape exhibited a severely degraded FWTM of 1683±81 ps in CTR, although the FWHM of 389±11 ps in the CTR has a similar range to the red or green PTFE tapes. The ESR film, while offering the best results for FWTM of 1121(±47) ps in CTR, had higher FWHM of 381(±13) ps in CTR than FWHM for the yellow PTFE tape.

As shown in Figure 3, for the yellow PTFE reflector, the cut-off wavelength is similar to the scintillation light emission peak of BGO. Thus scintillation photons emitted at wavelengths longer than the cut-off wavelength can be reflected at the crystal boundaries as much as

the white reflector, resulting in the least scintillation light loss (4.1%) compared to other colors, as shown in Section 3.2. In contrast, since more Cerenkov photons are produced at lower wavelengths, far fewer Cerenkov photons are reflected by the yellow tape than the white reflector for a given cut-off wavelength of the yellow reflector. As a result, photon transit time dispersion decreased, contributing to the improvement in the FWHM in CRT. In addition, the FWTM in CTR was still slightly better compared to the white PTFE reflector. However, the CTRs curves for the yellow and white PTFE tapes intersected each other below the FWTM lines. For the green, red, and black PTFE tapes, FWTMs in CTRs were degraded compared to the yellow reflector. However, based on the FWHMs in CTRs in Table 2, all colored reflectors show still better FWHMs in CTRs than the white PTFE reflector. Therefore, these results confirmed that reducing the number of reflections at the lateral sides improves timing performance by decreasing transit time dispersion of the fast Cerenkov photons. The improvement in timing resolution was different depending on the reflectance of the reflector. For the yellow, red, and black PTFE tapes, as the cut-off wavelength increases due to the color, FWTM values were degraded in the order of the color. One of the possible reasons is that since the number of Cerenkov photons reflected and arriving at the photosensor decreases, the probability that the Cerenkov photons are the first photons to be detected also decreases. When scintillation photons are more likely to be the first ones detected, the tails of the timing spectrum become longer, worsening FWTM in CTR (Kwon et al., 2019).

Additionally, we evaluated CTRs using two distinct energy windows (FWHM and FWTM) to investigate the dependency of timing performance on the energy window. With a few exceptions, notably the FWHM for the green PTFE tape and the FWTM for the ESR film, CTRs generally demonstrated slight improvements as the energy window narrowed from FWTM to FWHM. Notably, the yellow PTFE tape consistently shows lower FWHM values in CTRs compared to the white PTFE reflector for both energy windows, highlighting its superior performance.

Consequently, among the colored PTFE tapes studied, the yellow PTFE tape was the best reflector for better timing performance in the BGO pixel with minimum scintillation light loss compared to the conventional white PTFE reflector.

3.4   Additional discussion

There have been studies on various coating methods for scintillators to make the most of the emitted scintillation photons. However, most methods, such as distributed Bragg reflectors, metal coating, modified photonic crystal structures, and a high reflective film method, require special processing for scintillators, causing increased costs for implementation (Gramuglia et al., 2021; Xu et al., 2018). Furthermore, these methods have mostly focused on maximizing scintillation light collection without considering Cerenkov photons. Therefore, to be employed in our approach, these methods may require further studies.

By applying such discontinuous reflectance for the BGO reflector, the reflection of Cerenkov photons was effectively suppressed while minimizing scintillator light loss. The timing performance was much improved with the least energy performance degradation when yellow PTFE tape was employed. In addition, for the colored PTFE reflectors,

measurements with another SiPM type (NUV-HD-CHK, FBK, Italy) (Gundacker et al., 2023) were performed, which confirmed the trend of the best CTR 370 ps for the yellow reflector and the worst one for the white reflector (Lee et al., 2022). The proposed method is a straightforward and cost-effective method, and does not require additional signal processing or advanced preamplifier circuits to improve BGO time performance. Furthermore, the advantage of this method can be expanded to other applications that generate photons at different wavelength ranges.

In this study, we have used commercially available colored PTFE tapes. However, as the colors of reflectors can be changed or tuned using a mixture of different colors while manufacturing, it is highly likely that timing and energy performance may be further improved using reflectors with optimized spectral reflectance properties.

Lastly, our method employing yellow PTFE reflectors outperforms ESR film reflectors in terms of the FWHM of CTR, thereby validating the efficacy of our approach. However, an intriguing dynamic was observed: while the yellow PTFE reflector shows superior performance in terms of FWHM in CTR, the ESR film exhibits a slightly more favorable FWTM in CTR. These subtle yet significant differences raise questions about the better performer at the image level. As noted in previous discussions, including (Nuyts et al., 2022), a more comprehensive and in-depth analysis will indeed be required as we look toward color optimization at the image level.

4. Conclusion

This study showed that the timing performance of BGO-base TOF-PET detectors, which use Cerenkov photons for timing and scintillation photons for energy, can be improved by using discontinuous reflectance of colored PTFE tapes. Among the three commercially available colors (red, green, and yellow), when the yellow PTFE reflector was applied to the $3 \times 3 \times 20$ mm^3 BGO pixel, the FWHM of the CTR was improved by about 38 ps compared to the CTR from a convention white PTFE reflector. Moreover, the yellow tape also showed the least scintillation light loss compared to other colors. The 365±5 ps CTR of 20 mm long BGO pixels wrapped with yellow PTFE tape is the best achieved to data without using RF-based amplifiers, which typically require sophisticated design techniques for utilizing high-frequency signals. This method effectively enhanced timing performance with adequate energy information by only changing the color of the reflector from the conventional white without any additional circuitry for the BGO-based PET detector configuration.

Additional performance improvement may be expected by optimizing the colors of PTFE tape. PTFE reflectors may be inappropriate for array-type PET detector modules. Therefore, applying different colors for other reflector materials (barium sulfate, titanium dioxide, enhanced specular reflector, etc.) will be investigated for the best BGO reflector in future studies.

Acknowledgments

References

Brunner SE, & Schaart DR (2017). BGO as a hybrid scintillator / Cherenkov radiator for cost-effective time-of-flight PET. Physics in Medicine and Biology, 62(11), 4421–4439. 10.1088/1361-6560/aa6a49 [PubMed: 28358722]

Dolenec R, Korpar S, Križan P, Pestotnik R, & Verdel N (2016). The Performance of Silicon Photomultipliers in Cherenkov TOF PET. IEEE Transactions on Nuclear Science, 63(5), 2478–2481. 10.1109/TNS.2015.2512564

Dury MR, Theocharous T, Harrison N, Fox N, & Hilton M (2007). Common black coatings - reflectance and ageing characteristics in the 0.32-14.3 μm wavelength range. Optics Communications, 270(2), 262–272. 10.1016/j.optcom.2006.08.038

Gilbert PUPA, & Haeberli W (2007). Experiments on subtractive color mixing with a spectrophotometer. American Journal of Physics, 75(4), 313–319. 10.1119/1.2431654

Gola A, Piemonte C, & Tarolli A (2013). Analog circuit for timing measurements with large area sipms coupled to lyso crystals. IEEE Transactions on Nuclear Science, 60(2), 1296–1302. 10.1109/TNS.2013.2252196

Gonzalez-Montoro A, Pourashraf S, Cates JW, & Levin CS (2022). Cherenkov Radiation-Based Coincidence Time Resolution Measurements in BGO Scintillators. Frontiers in Physics, 10. 10.3389/fphy.2022.816384

Gonzalez-Montoro A, Pourashraf S, Lee MS, Cates JW, & Levin CS (2021). Study of optical reflectors for a 100ps coincidence time resolution TOF-PET detector design. Biomedical Physics and Engineering Express, 7(6). 10.1088/2057-1976/ac240e

Gramuglia F, Frasca S, Ripiccini E, Venialgo E, Gâté V, Kadiri H, Descharmes N, Turover D, Charbon E, & Bruschini C (2021). Light extraction enhancement techniques for inorganic scintillators. Crystals, 11(4). 10.3390/cryst11040362

Gundacker S, Borghi G, Cherry SR, Gola A, Lee D, Merzi S, Penna M, Schulz V, & Kwon SI (2023). On timing-optimized SiPMs for Cherenkov detection to boost low cost time-of-flight PET. Physics in Medicine & Biology 10.1088/1361-6560/ace8ee

Gundacker S, Martinez Turtos R, Kratochwil N, Pots RH, Paganoni M, Lecoq P, & Auffray E (2020). Experimental time resolution limits of modern SiPMs and TOF-PET detectors exploring different scintillators and Cherenkov emission. Physics in Medicine and Biology, 65(2). 10.1088/1361-6560/ab63b4

Janecek M (2012). Reflectivity spectra for commonly used reflectors. IEEE Transactions on Nuclear Science, 59(3 PART 1), 490–497. 10.1109/TNS.2012.2183385

Karp JS, Surti S, Daube-Witherspoon ME, & Muehllehner G (2008). Benefit of time-of-flight in PET: Experimental and clinical results. Journal of Nuclear Medicine, 49(3), 462–470. 10.2967/jnumed.107.044834 [PubMed: 18287269]

Kratochwil N, Gundacker S, Lecoq P, & Auffray E (2020). Pushing Cherenkov PET with BGO via coincidence time resolution classification and correction. Physics in Medicine and Biology, 65(11). 10.1088/1361-6560/ab87f9

Kwon SI, Gola A, Ferri A, Piemonte C, & Cherry SR (2016). Bismuth germanate coupled to near ultraviolet silicon photomultipliers for time-of-flight PET. Physics in Medicine and Biology, 61(18), L38–L47. 10.1088/0031-9155/61/18/L38 [PubMed: 27589153]

Kwon SI, Roncali E, Gola A, Paternoster G, Piemonte C, & Cherry SR (2019). Dual-ended readout of bismuth germanate to improve timing resolution in time-of-flight PET. Physics in Medicine and Biology, 64(10). 10.1088/1361-6560/ab18da

Lecoq P, Auffray E, Brunner S, Hillemanns H, Jarron P, Knapitsch A, Meyer T, & Powolny F (2010). Factors influencing time resolution of scintillators and ways to improve them. IEEE Transactions on Nuclear Science, 57(5 PART 1), 2411–2416. 10.1109/TNS.2010.2049860

Leem H, Choi Y, Jung J, Park K, Kim Y, & Jung JH (2022). Optimized TOF-PET detector using scintillation crystal array for brain imaging. Nuclear Engineering and Technology, 54(7), 2592–2598. 10.1016/j.net.2022.02.009

Lowdon M, Martin PG, Hubbard MWJ, Taggart MP, Connor DT, Verbelen Y, Sellin PJ, & Scott TB (2019). Evaluation of scintillator detection materials for application within airborne environmental radiation monitoring. Sensors (Switzerland), 19(18). 10.3390/s19183828

Merzi S, Brunner SE, Gola A, Inglese A, Mazzi A, Paternoster G, Penna M, Piemonte C, & Ruzzarin M (2023). NUV-HD SiPMs with metal-filled trenches. Journal of Instrumentation, 18(5). 10.1088/1748-0221/18/05/P05040

Moses WW (n.d.). Recent Advances and Future Advances in Time-of-Flight PET

Nuyts J, Defrise M, Gundacker S, Roncali E, & Lecoq P (2022). The SNR of positron emission data with Gaussian and non-Gaussian time-of-flight kernels, with application to prompt photon coincidence. IEEE Transactions on Medical Imaging 10.1109/TMI.2022.3225433

Romanchek G, Wang Y, Marupudi H, & Abbaszadeh S (2020). Performance of optical coupling materials in scintillation detectors post temperature exposure. In Sensors (Switzerland) (Vol. 20, Issue 21, pp. 1–13). MDPI AG. 10.3390/s20216092

Roncali E, Kwon SI, Jan S, Berg E, & Cherry SR (2019). Cerenkov light transport in scintillation crystals explained: Realistic simulation with GATE. Biomedical Physics and Engineering Express, 5(3). 10.1088/2057-1976/ab0f93

Roncali E, Stockhoff M, & Cherry SR (2017). An integrated model of scintillator-reflector properties for advanced simulations of optical transport. Physics in Medicine and Biology, 62(12), 4811–4830. 10.1088/1361-6560/aa6ca5 [PubMed: 28398905]

Sattar S (2019). Characterizing Color with Reflectance. Journal of Chemical Education, 96(6), 1124–1128. 10.1021/acs.jchemed.8b00845

Seitz B, Campos Rivera N, & Stewart AG (2016). Energy Resolution and Temperature Dependence of Ce:GAGG Coupled to 3 mm × 3 mm Silicon Photomultipliers. IEEE Transactions on Nuclear Science, 63(2), 503–508. 10.1109/TNS.2016.2535235

Surti S (2015). Update on time-of-flight PET imaging. Journal of Nuclear Medicine, 56(1), 98–105. 10.2967/jnumed.114.145029 [PubMed: 25525181]

Surti S, & Karp JS (2016). Advances in time-of-flight PET. In Physica Medica (Vol. 32, Issue 1, pp. 12–22). Associazione Italiana di Fisica Medica. 10.1016/j.ejmp.2015.12.007 [PubMed: 26778577]

Szczesniak T, Kapusta M, Moszynski M, Grodzicka M, Szawlowski M, Wolski D, Baszak J, & Zhang N (2013). MPPC arrays in PET detectors with LSO and BGO scintillators. IEEE Transactions on Nuclear Science, 60(3), 1533–1540. 10.1109/TNS.2013.2251002

Trigila C, Ariño-Estrada G, Kwon SI, & Roncali E (2022). The Accuracy of Cerenkov Photons Simulation in Geant4/Gate Depends on the Parameterization of Primary Electron Propagation. Frontiers in Physics, 10. 10.3389/fphy.2022.891602

Ullah MN, Pratiwi E, Cheon J, Choi H, & Yeom JY (2016). Instrumentation for Time-of-Flight Positron Emission Tomography. In Nuclear Medicine and Molecular Imaging (Vol. 50, Issue 2, pp. 112–122). Springer Verlag. 10.1007/s13139-016-0401-5 [PubMed: 27275359]

Vandenberghe S, Mikhaylova E, D'Hoe E, Mollet P, & Karp JS (2016). Recent developments in time-of-flight PET. In EJNMMI Physics (Vol. 3, Issue 1). Springer International Publishing. 10.1186/s40658-016-0138-3

Weber S, Christ D, Kurzeja M, Engels R, Kemmerling G, & Halling H (2003). Comparison of LuYap, LSO, and BGO as Scintillators for High Resolution PET Detectors. IEEE Transactions on Nuclear Science, 50(5 II), 1370–1372. 10.1109/TNS.2003.817952

Xu J, Sun Q, Wu Z, Guo L, Xie S, Huang Q, & Peng Q (2018). Development of broad-band high-reflectivity multilayer film for positron emission tomography system. Journal of Instrumentation, 13(9). 10.1088/1748-0221/13/09/P09016

Lee D, Cherry S, & Kwon SI (2022). Colored reflectors to improve timing resolution of BGO-based time-of-flight PET detectors, Journal of Nuclear Medicine June 2022, 63 (supplement 2) 2342

Figure 1.
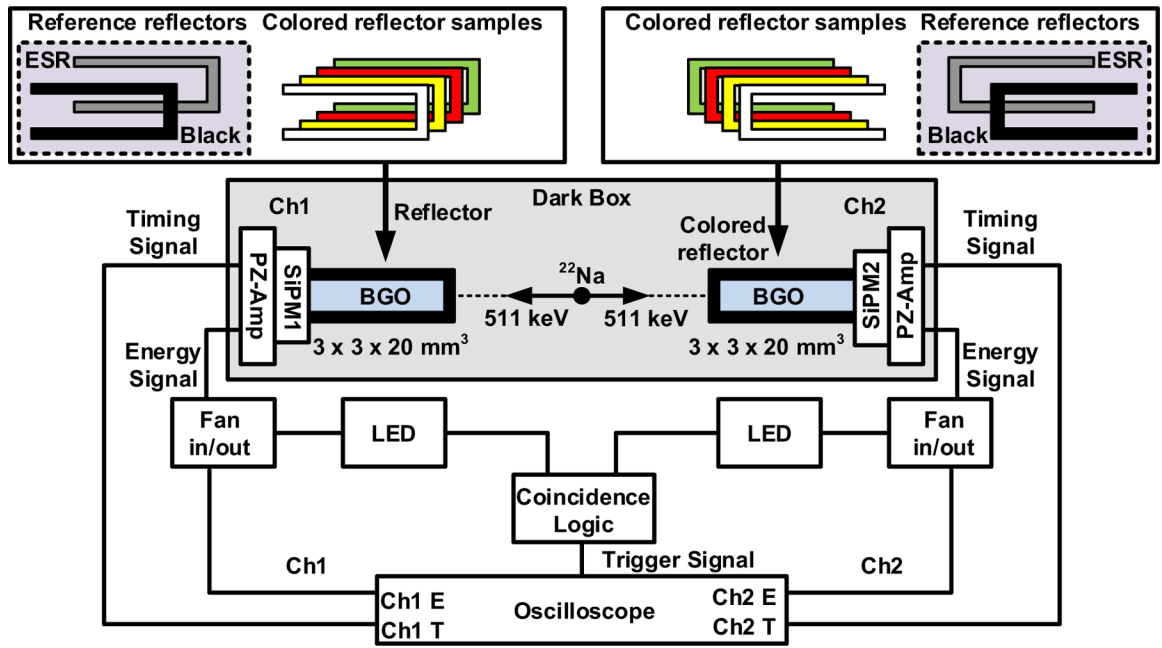White and three different colored (yellow, green, and red) PTFE tapes used for the BGO
pixel reflector.

Figure 2.
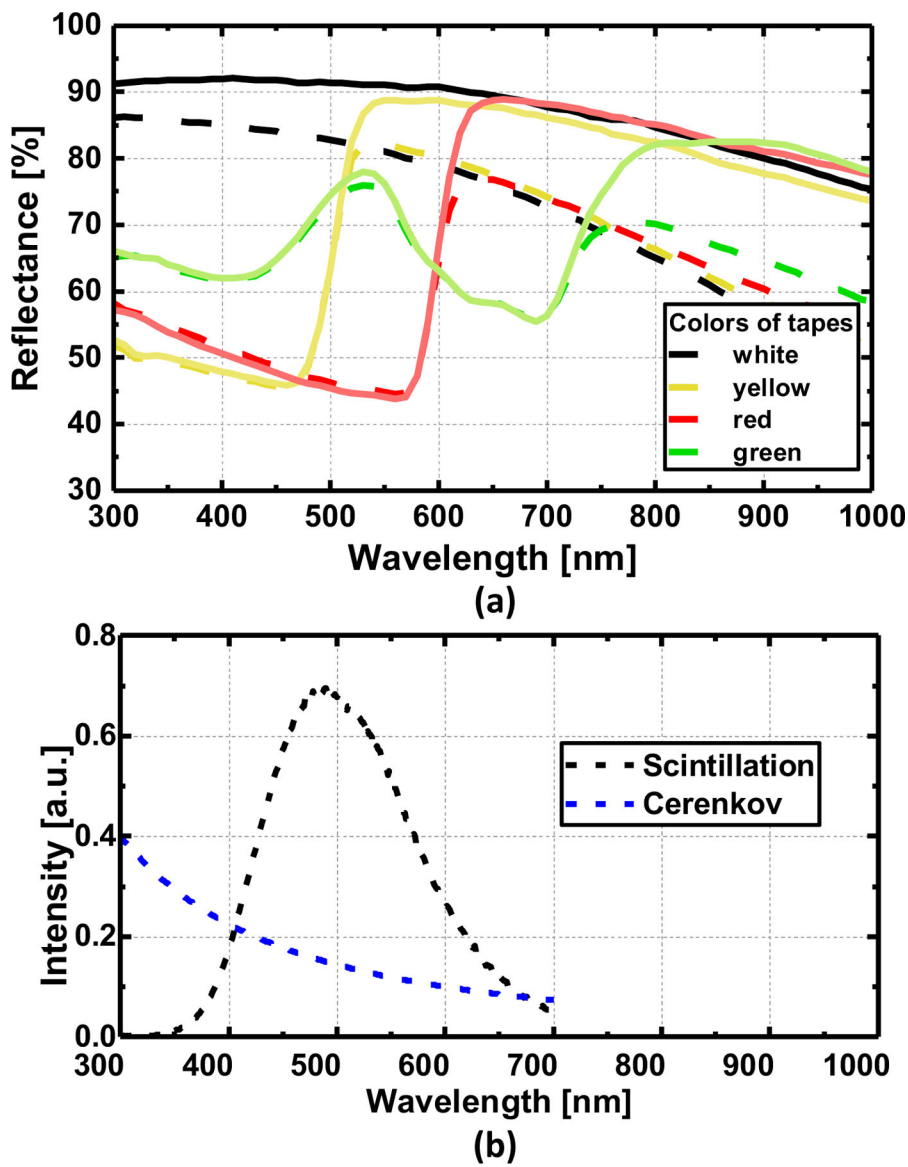Experimental setup for coincidence measurements

Figure 3.
Measured reflectance of single-layer (dashed-line) and three-layer (solid-line) colored PTFE tapes (a), and BGO scintillation and Cerenkov light spectra as a function of wavelength (b)
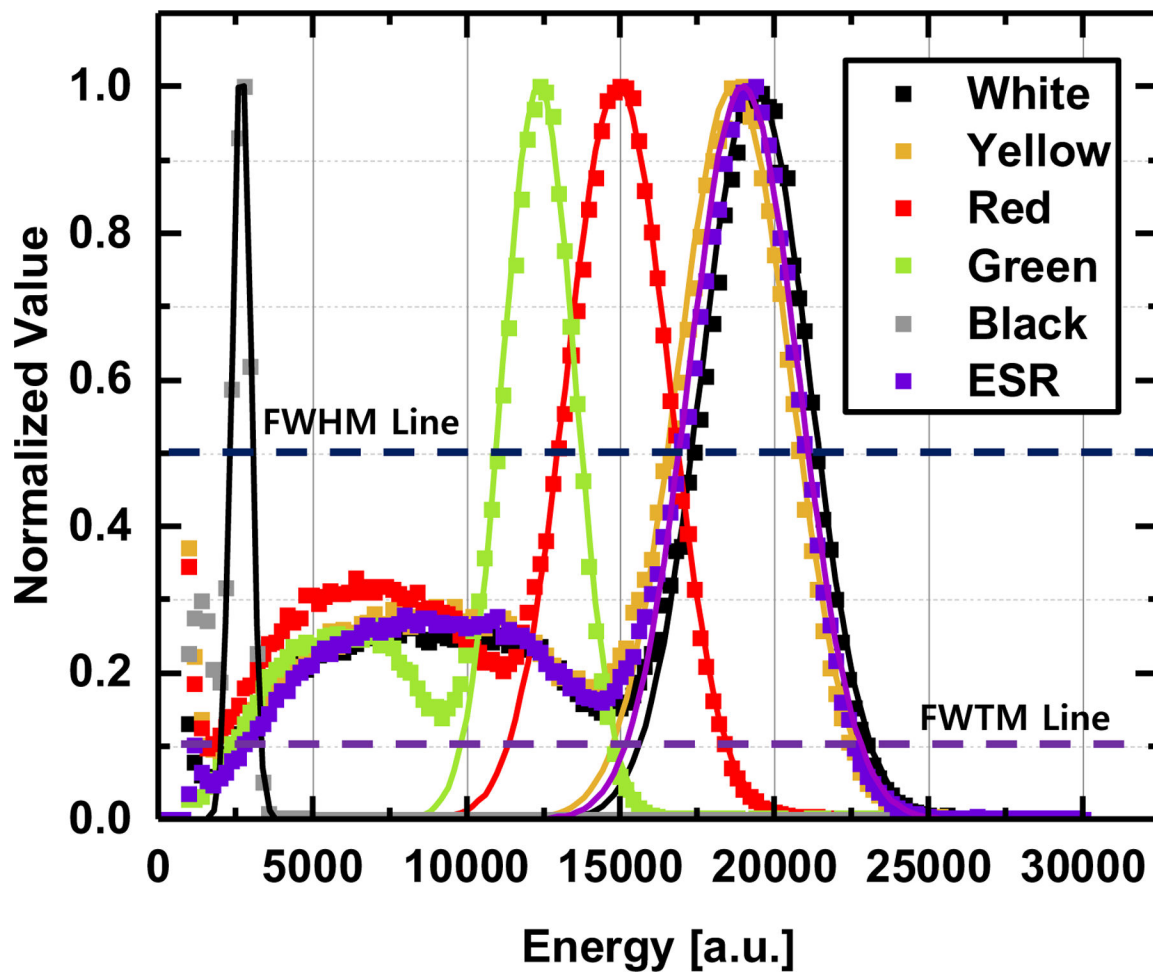
Figure 4.
Energy spectra for different reflectors (acquired in coincidence) obtained from a $3 \times 3 \times 20$ mm^3 BGO pixel, together with the Gaussian fits and FWHM and FWTM lines for energy window.
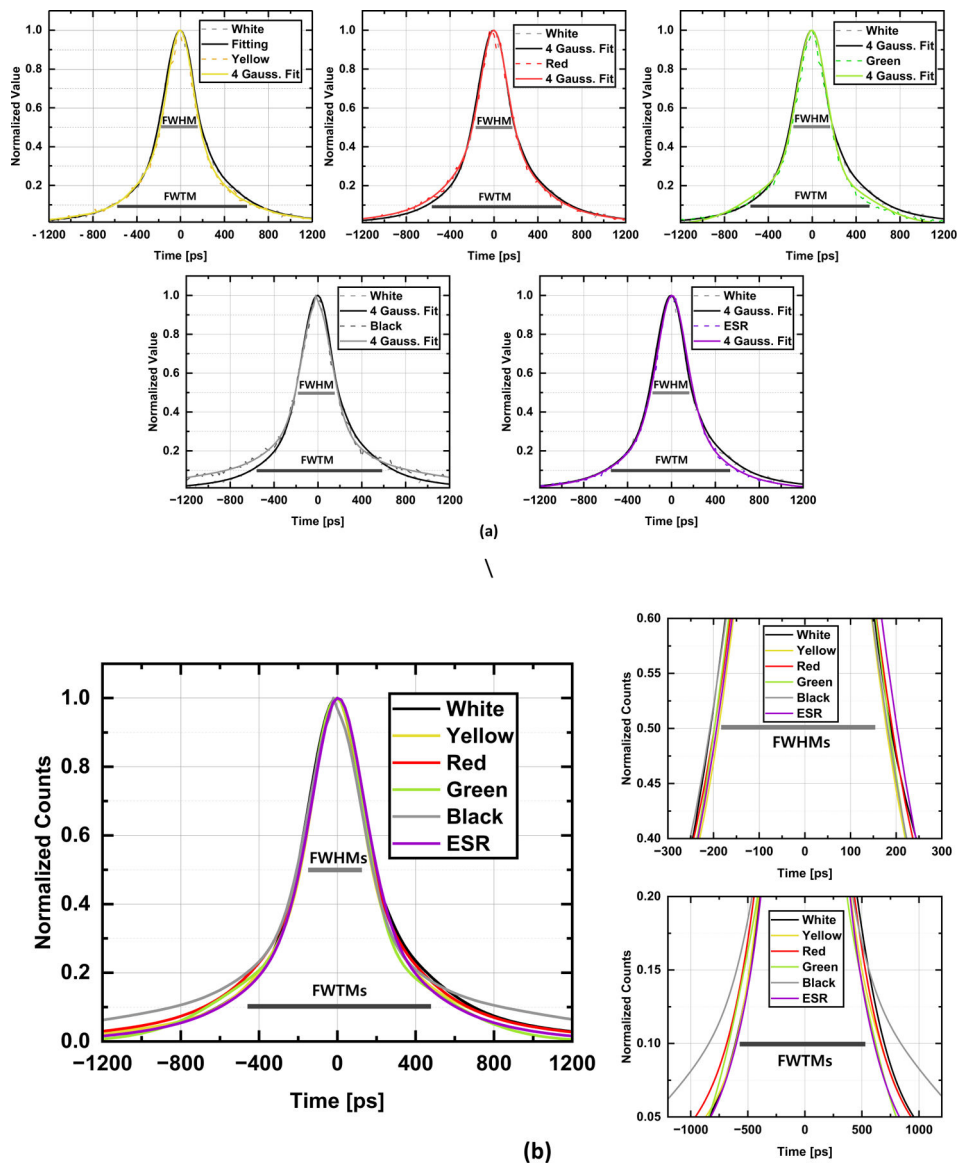
Figure 5.
Coincidence timing spectra for different reflectors applied to $3 \times 3 \times 20$ mm^3 BGO pixels (a). Comparison of fitted timing spectra for the different reflectors (b)

Table 1.

Photopeak position and energy resolution for each reflector

Reflectors	Photopeak($\times 10^3$)	Energy resolution[%]
White PTFE	19.4	21.4
Yellow PTFE	18.6	23.2
Red PTFE	15.0	26.3
Green PTFE	12.4	23.6
Black painted PTFE	2.8	28.0
ESR	18.9	22.2

Table 2.

Coincidence timing resolution (CTR) obtained from each measurement with different energy window ranges: FWTM and FTHM.

Reflectors	Energy Window FWTM		Energy Window FWHM	
	CTR FWHM [ps]	CTR FWTM [ps]	CTR FWHM [ps]	CTR FWTM [ps]
White PTFE	403±14	1309±31	394±21	1314±80
Yellow PTFE	365±5	1269±34	361±3	1213±20
Red PTFE	388±14	1352±46	380±14	1313±54
Green PTFE	383±3	1287±22	391±12	1171±41
Black painted PTFE	389±11	1683±81	388±16	1655±99
ESR	381±13	1121±47	378±12	1139±48